Uterine ALK3 is essential during the window of implantation

Diana Monsivais[a,b,1], Caterina Clementi[a,1,2], Jia Peng[a,3], Mary M. Titus[a], James P. Barrish[c], Chad J. Creighton[d,e], John P. Lydon[b,f], Francesco J. DeMayo[g], and Martin M. Matzuk[a,b,e,f,h,i,j,4]

[a]Department of Pathology and Immunology, Baylor College of Medicine, Houston, TX 77030; [b]Center for Reproductive Medicine, Baylor College of Medicine, Houston, TX 77030; [c]Electron Microscopy Laboratory, Texas Children's Hospital, Houston, TX 77030; [d]Department of Medicine, Baylor College of Medicine, Houston, TX 77030; [e]Dan L. Duncan Comprehensive Cancer Center, Baylor College of Medicine, Houston, TX 77030; [f]Department of Molecular and Cellular Biology, Baylor College of Medicine, Houston, TX 77030; [g]National Institute of Environmental Health Sciences, Research Triangle Park, NC 27709; [h]Department of Molecular and Human Genetics, Baylor College of Medicine, Houston, TX 77030; [i]Department of Pharmacology, Baylor College of Medicine, Houston, TX 77030; and [j]Center for Drug Discovery, Baylor College of Medicine, Houston, TX 77030

Contributed by Martin M. Matzuk, December 3, 2015 (sent for review October 27, 2015; reviewed by Indrani C. Bagchi and Bruce D. Murphy)

The window of implantation is defined by the inhibition of uterine epithelial proliferation, structural epithelial cell remodeling, and attenuated estrogen (E2) response. These changes occur via paracrine signaling between the uterine epithelium and stroma. Because implantation defects are a major cause of infertility in women, identifying these signaling pathways will improve infertility interventions. Bone morphogenetic proteins (BMPs) are TGF-β family members that regulate the postimplantation and midgestation stages of pregnancy. In this study, we discovered that signaling via activin-like kinase 3 (ALK3/BMPR1A), a BMP type 1 receptor, is necessary for blastocyst attachment. Conditional knockout (cKO) of ALK3 in the uterus was obtained by producing *Alk3*$^{flox/flox}$-*Pgr-cre*–positive females. *Alk3* cKO mice are sterile and have defects in the luminal uterine epithelium, including increased microvilli density and maintenance of apical cell polarity. Moreover, *Alk3* cKO mice exhibit an elevated uterine E2 response and unopposed epithelial cell proliferation during the window of implantation. We determined that dual transcriptional regulation of Kruppel-like factor 15 (*Klf15*), by both the transforming growth factor β (TGF-β) transcription factor SMAD family member 4 (SMAD4) and progesterone receptor (PR), is necessary to inhibit uterine epithelial cell proliferation, a key step for embryo implantation. Our findings present a convergence of BMP and steroid hormone signaling pathways in the regulation of uterine receptivity.

BMP signaling pathway | endometrium | implantation failure | infertility | progesterone receptor

Drastic structural and molecular changes are necessary for the luminal uterine epithelium to achieve a receptive status. Because it is the first site of contact between the mother and the invading blastocyst, remodeling of the luminal epithelium is crucial for establishing a successful pregnancy (1, 2). The steroid hormones, estrogen (E2) and progesterone (P4), coordinate many of these changes; however, many other growth factors and cytokines are involved (3, 4). The bone morphogenetic proteins (BMPs) are a class of growth factors that are important during pregnancy. BMPs are members of the transforming growth factor β (TGF-β) signaling pathway that regulate many cellular pathways, including processes related to normal reproductive function and pregnancy (5–13). BMPs transmit their signals by binding to a cell surface heterodimeric receptor complex that is composed of a combination of two type 1 receptors [activin-like kinase 2 (ALK2), ALK3, or ALK6] and two type 2 receptors [activin A receptor type II A (ACVR2A), ACVR2B, or BMP type 2 receptor (BMPR2)] (14–16). Upon ligand binding, the heterodimeric BMP receptor complex signals by phosphorylating and activating SMAD1/5/8, which associate with SMAD family member 4 (SMAD4) and translocate to the nucleus to regulate gene expression (17).

BMPs are expressed in a temporal manner throughout early and late pregnancy (18), and conditional deletion of BMP2 results in female infertility due to failed decidualization of the endometrial stroma (12, 19). Conditional deletion of the BMPR1, ALK2, results in female infertility due to impaired endometrial stromal cell decidualization that abrogates pregnancy in the postimplantation period (11). Conditional deletion of the BMPR2 also results in female infertility; these mice have defective spiral artery remodeling during the midgestation period that results in intrauterine growth restriction; implantation site hemorrhage; and, ultimately, fetal death (13). Despite the crucial roles for ALK2 and BMPR2 during the postimplantation stages, the specific BMP ligands and receptors that coordinate blastocyst attachment are not yet known.

Decreased uterine response to E2 determines receptivity during the window of implantation. Because tightly regulated levels of E2 are required for successful implantation (20), dynamic epithelial-stromal communication is crucial during this period. Paracrine signaling pathways, such as the paracrine signaling pathways regulated by Indian hedgehog (IHH)/chicken ovalbumin upstream promoter transcription factor II (COUP-TFII) (21, 22) or heart and neural crest derivatives expressed 2 (HAND2) (23), suppress E2-mediated actions in the luminal epithelium during the

Significance

In the assisted reproductive technology (ART) clinic, pregnancy is defined by the rise of human chorionic gonadotropin upon embryo implantation. Achieving embryo implantation is a major roadblock to the success of ART; it is estimated that only 50% of transferred embryos implant in patients seeking ART, and that half of these embryos are subsequently lost. Thus, understanding the molecular pathways during the window of implantation will improve ART success. In this study, we conditionally deleted activin-like kinase 3 (ALK3) in mice and demonstrate that bone morphogenetic protein (BMP) signaling via ALK3 defines uterine receptivity. This mouse model will be a valuable research tool for studying implantation failure in women, and the results herein will contribute to our knowledge regarding female infertility.

Author contributions: D.M., C.C., J.P., M.M.T., J.P.B., C.J.C., J.P.L., F.J.D., and M.M.M. designed research; D.M., C.C., J.P., M.M.T., J.P.B., C.J.C., and M.M.M. performed research; D.M., C.C., J.P., C.J.C., J.P.L., F.J.D., and M.M.M. analyzed data; and D.M., C.C., J.P., M.M.T., C.J.C., J.P.L., F.J.D., and M.M.M. wrote the paper.

Reviewers: I.C.B., University of Illinois at Urbana–Champaign; and B.D.M., University of Montreal.

The authors declare no conflict of interest.

Data deposition: The data reported in this paper have been deposited in the Gene Expression Omnibus (GEO) database, www.ncbi.nlm.nih.gov/geo (accession no. GEO73717).

[1]D.M. and C.C. contributed equally to this work.

[2]Present address: Celmatix Inc., New York, NY 10005.

[3]Present address: Department of Molecular Biology, Princeton University, Princeton, NJ 08544.

[4]To whom correspondence should be addressed. Email: mmatzuk@bcm.edu.

This article contains supporting information online at www.pnas.org/lookup/suppl/doi:10.1073/pnas.1523758113/-/DCSupplemental.

process of implantation (21–23). The proliferative response to E2 is also regulated by the transcription factors Kruppel-like factor 4 (KLF4) and KLF15 (24). The KLFs are evolutionary conserved DNA binding proteins with diverse roles in development and physiology (25). Previous studies revealed that *Klf15* is a direct target of progesterone receptor (PR), whereas *Klf4* expression is up-regulated by E2 in the mouse uterus (24, 26). During proestrus, the elevated levels of circulating E2 maintain uterine epithelial cell proliferation through the activation of KLF4. KLF4 binds to the promoter of Minichromosome maintenance-2 (*Mcm2*) and induces its expression, resulting in cell cycle progression from G1 to S phase. Following the postcopulatory surge of P4, KLF15 expression is induced and inhibits uterine epithelial proliferation by repressing *Mcm2* expression (24). Thus, the uterine response to E2 and P4 is regulated by a host of transcription factors that are activated spatiotemporally during the reproductive cycle.

Highly coordinated molecular pathways are necessary to achieve normal blastocyst attachment. Previous studies from our laboratory and other laboratories indicate that the BMP signaling pathway is a major regulator of the pathways that control pregnancy (11–13). Here, we demonstrate that ALK3, a BMPR1, is a key regulator of blastocyst attachment. Because *Alk3* null mice are embryonic lethal at embryonic day 9.5 due to failed mesoderm formation (27), we conditionally deleted *Alk3* in PR-expressing tissues by mating $Alk3^{flox/flox}$ females (28) to males with a *Pgr-cre* (29) knock-in allele to produce, eventually, *Alk3* conditional knockout (cKO) females. Compared with control females, we discovered that *Alk3* cKO females are sterile due to failed blastocyst attachment. Molecular analyses during the window of implantation reveal that *Alk3* cKO mice have severe defects in the uterine luminal epithelium that abrogate blastocyst attachment.

Although the use of assisted reproductive technology (ART) has greatly increased since the birth of the first child was achieved through in vitro fertilization in 1978, the success rate of live births using ART remains low (30). Several factors contribute to female infertility, yet it is thought that failed implantation accounts for ∼75% of failed pregnancies (31, 32). Our current examination of the *Alk3* cKO mice indicates that characterization and understanding of the BMP ligands, BMPRs, and downstream gene targets hold the potential for novel therapeutic targets and strategies for female infertility.

Results

Conditional Deletion of Alk3 Results in Female Infertility. We determined that ALK3 is expressed throughout early pregnancy in the mouse uterus and that its expression peaks at 3.5 d postcoitus (dpc) (Fig. S1). Given that *Alk3* null mice are embryonically lethal (27, 28), we generated conditional mutant mice by mating $Alk3^{flox/flox}$ females (28) to $Alk3^{flox/flox}$-*Pgr-cre* males (Fig. 1*A*). This breeding strategy allowed us to study the role of ALK3 in the *Pgr*-expressing tissues of the female reproductive tract (ovaries, uterus, and oviduct) (29). We first assessed the effectiveness of ALK3 recombination in the uterus by immunofluorescence and quantitative RT-PCR (qRT-PCR). *Alk3* expression was significantly decreased in the uterus of *Alk3* cKO mice (Fig. 1*B*), indicating successful ALK3 deletion. Fig. 1*C* demonstrates that although *Alk3* was readily detected in the uterine stroma and luminal epithelium of the control mice, ALK3 immunoreactivity was absent in the *Alk3* cKO mice. We performed a 6-mo fertility trial, which indicated that although each control female gave birth to 58 ± 8.1 offspring, *Alk3* cKO female mice were sterile (Table 1). We concluded that ALK3 is essential for female reproductive function.

To determine whether the infertility of *Alk3* cKO mice was the result of ovarian defects, we assessed ovarian function using various parameters. Ovarian transplants were performed between WT-WT, WT-cKO, and cKO-WT mice (Table S1). WT recipients with WT or *Alk3* cKO donor ovaries delivered pups; however, none of the cKO recipient mice with WT ovaries delivered pups, indicating

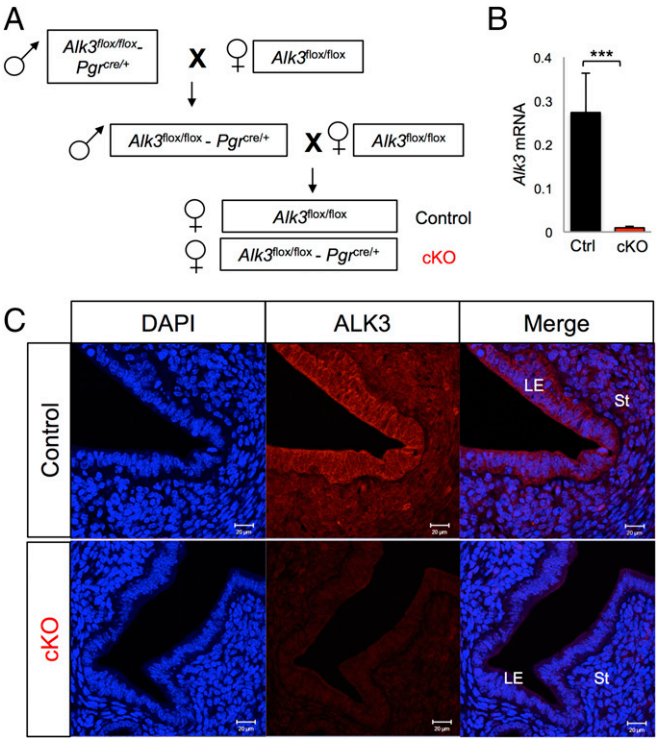

Fig. 1. Generating mice with conditional deletion of ALK3. (*A*) Breeding scheme used to generate *Alk3* cKO female mice. (*B*) Expression of uterine *Alk3* was quantified using qRT-PCR in the uteri of control (Ctrl) and *Alk3* cKO mice ($n = 4$). (*C*) Immunofluorescence of ALK3 in the uterus of control (*Top*) and *Alk3* cKO (*Bottom*) mice at 3.5 dpc. (Scale bars: 20 μM.) LE, luminal epithelium; St, stroma. ***$P < 0.0001$. Data are mean ± SEM.

normal ovarian function in *Alk3* cKO mice. Likewise, serum hormone levels collected from mice at 3.5 dpc indicated no significant differences in the circulating levels of estradiol (3.75 pg/mL ± 0.31 in controls vs. 4.23 pg/mL ± 0.38 in *Alk3* cKO mice) or P4 (21.11 ng/mL ± 3.24 in controls vs. 20.65 ng/mL ± 3.07 in *Alk3* cKO mice) (Fig. S2 *A* and *B*). Gonadotropin stimulation of sexually immature mice with pregnant mare serum gonadotropin (PMSG) induced follicle maturation equally in *Alk3* controls and *Alk3* cKO mice, indicating normal ovarian follicle maturation in the cKO mice (Fig. S2 *C* and *D*). These results indicated that the infertility observed in *Alk3* cKO mice was due to uterine or oviductal defects.

After ovulation, unfertilized eggs enter the oviduct, where fertilization occurs if mating occurred (3). To assess whether oviduct function was compromised in the cKOs, we measured the response to superovulation, quantified the fertilization rate, and assessed blastocyst formation in control and *Alk3* cKO female mice. No differences in any of these parameters were observed (Fig. S2 *E*–*G*), indicating that conditional deletion of *Alk3* with *Pgr-cre* did not interfere with oocyte quality or fertilization. Overall, we determined that the infertility in *Alk3* cKO mice did not affect ovarian or oviductal function.

Defective Embryo Attachment and Decidualization in the Uterus of Alk3 cKO Mice. Because normal ovarian and oviductal function was observed in the *Alk3* cKO mice, we hypothesized that uterine defects would be the major cause of infertility. We determined that blastocyst implantation was defective in *Alk3* cKO mice by using vascular blue dye injection at 4.5 dpc to visualize implantation sites in the uterus (Fig. 2 *A* and *B*). Although numerous implantation sites were observed in the control mice (Fig. 2*A*), implantation sites were completely absent in the *Alk3* cKO mice (Fig. 2*B*). In mice, blastocyst apposition and attachment

Table 1. Six-month fertility trial demonstrates that *Alk3* cKO females are sterile

Genotype	No. of mice, *n*	Pups per litter	Pups born per female in 6 mo
Alk3$^{flox/flox}$	10	9.0 ± 0.8	58 ± 8.1
Alk3$^{flox/flox}$-*Pgr*^{cre}	10	0	0

occur on day 4 of pregnancy, at which point blastocysts can no longer be flushed from the uterus (33–35). We tested whether defective blastocyst attachment was occurring by mating *Alk3* cKO females to males carrying a transgene of the EGFP to visualize GFP-expressing embryos (Fig. S3*A*). We observed that GFP-expressing embryos were entirely flushed from the uterine lumen of *Alk3* cKO mice at 4.5 dpc, whereas most embryos remained attached to the uteri of the control mice (Fig. S3 *B* and *C*). We concluded that infertility in the *Alk3* cKO mice was likely the result of defective blastocyst attachment.

We analyzed the uteri of control and *Alk3* cKO mice on day 4.5 to characterize implantation. In contrast to control mice, which showed attached embryos (Fig. 2 *C* and *D*), complete luminal closure, and formation of the primary decidual zone, *Alk3* cKO mice had defective embryo attachment with incomplete luminal closure (Fig. 2 *E* and *F*). We also saw fewer decidual cells in the *Alk3* cKO mouse uterus compared with the controls (Fig. 2 *D* and *F*, indicated by white arrowheads), which gave rise to a reduced primary decidual zone compared with controls. This result indicated that unlike embryos in the control mice, embryos in the *Alk3* cKO mice did not fully attach or penetrate the luminal uterine epithelium. Thus, in addition to inhibiting blastocyst attachment, the absence of BMP signals mediated via ALK3 blunted the decidual response in the *Alk3* cKO mice.

It was previously determined that cyclooxygenase 2 (COX2) expression correlated with embryo implantation and that implantation was abrogated in *Cox2* null mice (36). We assessed whether COX2 expression would be present in the uteri of control and *Alk3* cKO mice at 4.5 dpc (Fig. 2 *G–J*). Compared with the control mice, where COX2 expression was strongly detected in the subepithelial stroma surrounding the embryo (Fig. 2 *G–H*), only weak COX2 expression was detected in the *Alk3* cKO mice (Fig. 2 *I* and *J*). Accordingly, the expression levels of various implantation-associated genes, including epiregulin (*Ereg*), *Cox2*, wingless-type MMTV integration site family member 4 (*Wnt4*), and *Bmp2*, were significantly decreased in the *Alk3* cKO uteri at 4.5 dpc (Fig. 2*K*). We also detected enhanced E2 response in the uteri of cKOs at 4.5 dpc (Fig. 2*K*), as shown by increased expression of fibroblast growth factor 9 (*Fgf9*), lipocalin 2 (*Lcn2*), and lactoferrin (*Ltf*). Overall, these results confirmed defective blastocyst implantation in the *Alk3* cKO mice.

In mice, decidualization of the endometrial stroma occurs in response to mechanical and growth factor signaling elicited by the implanting embryo (37). Endometrial stromal cell decidualization can be artificially induced in mice with a mechanical trauma to the uterus (38). We tested the response of control and *Alk3* cKO mice to the mechanical induction of decidualization (Fig. S4). Control and *Alk3* cKO mice were ovariectomized and treated with hormones as indicated in Fig. S4*A*, followed by the induction of a mechanical stimulus to one uterine horn to mimic decidualization. After 5 d, uterine horns were collected and processed for histology.

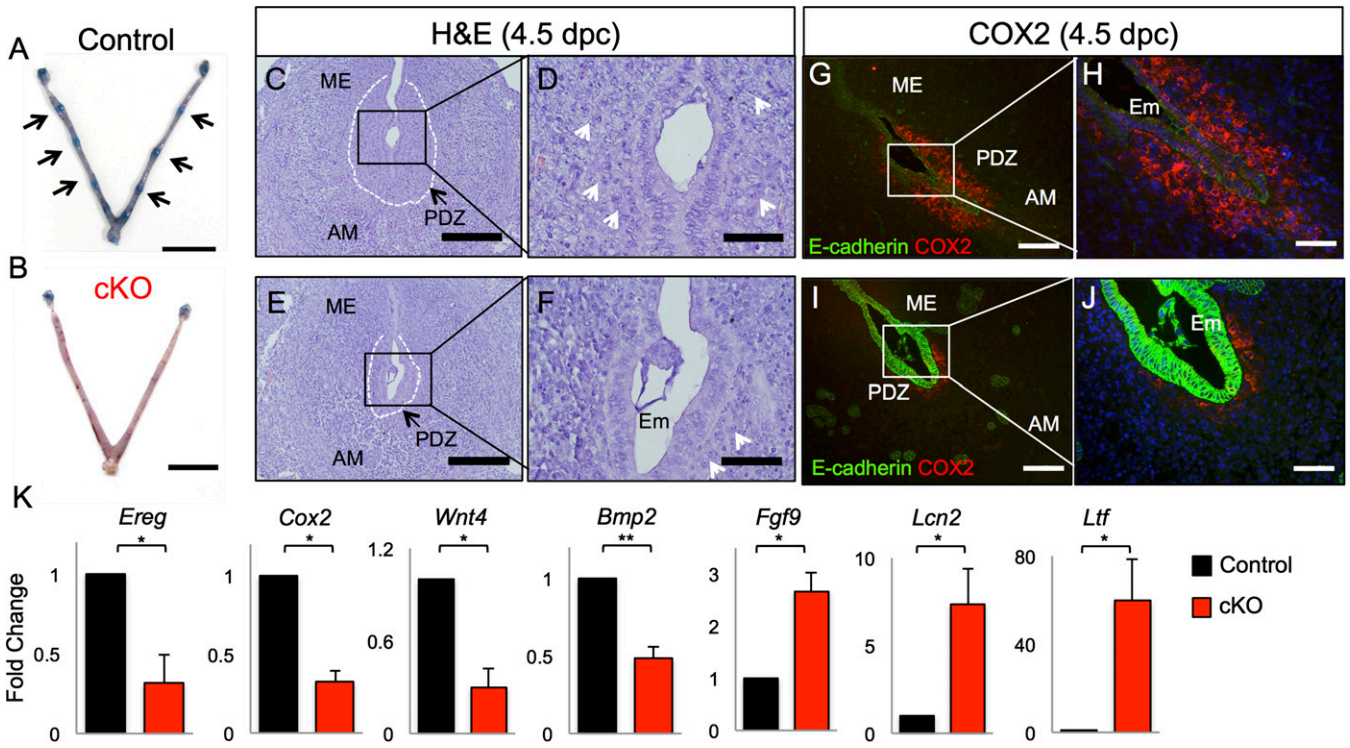

Fig. 2. Conditional deletion of ALK3 impairs blastocyst implantation and uterine decidualization. Implantation sites at 4.5 dpc (black arrows) were visualized by Chicago Blue vascular dye injection in control (*A*) and *Alk3* cKO (*B*) mice. (Scale bars: 1 cm.) H&E staining was performed in the uteri of 4.5-dpc control (*C* and *D*) and *Alk3* cKO mice (*E* and *F*). (Scale bars: lower magnification, 200 μM; higher magnification, 50 μM.) Immunofluorescence of COX2 (red) and E-cadherin (green) in the 4.5-dpc uterus of control (*G* and *H*) and *Alk3* cKO (*I* and *J*) mice is shown. (Scale bars: lower magnification, 100 μM; higher magnification, 50 μM.) (*K*) qRT-PCR analysis of implantation-related genes (*Ereg*, *Cox2*, *Wnt4*, and *Bmp2*) and E2-regulated genes (*Fgf9*, *Lcn2*, and *Ltf*) in control and *Alk3* cKO uteri at 4.5 dpc ($n = 4$). AM, antimesometrial; Em, embryo; ME, mesometrial; PDZ, primary decidual zone (outlined by white dashed line). White arrowheads indicate decidual cells. *$P < 0.05$; **$P < 0.001$. Data are mean ± SEM.

Compared with the enlarged uterine horns of control mice (Fig. S4*B*), the uterine horns of *Alk3* cKO mice did not decidualize (Fig. S4*C*). We also observed the presence of decidual cells and alkaline phosphatase activity in the decidualized horn of control mice (Fig. S4 *D* and *F*), but not in *Alk3* cKO mice (Fig. S4 *E* and *G*), indicating that ALK3 is necessary for endometrial stromal cell decidualization.

Defective Uterine Luminal Epithelium in Alk3 cKO Mice. To understand the role of ALK3 in the luminal uterine epithelium, we obtained the gene expression profiles of isolated luminal uterine epithelium from 3.5-dpc control and *Alk3* cKO mice (Fig. S5*A*). We assessed the purity of the isolated epithelial cells by staining with cytokeratin 8 (KRT8) and vimentin (VIM) antibodies (Fig. S5 *B* and *C*), and by measuring *Krt18* and *Vim* expression with qRT-PCR (Fig. S5 *D* and *E*). Microarray profiling demonstrated that 439 gene probes were differentially expressed between the control and *Alk3* cKO mice (Fig. S5*F*; <0.7, >1.5-fold change, $P < 0.05$). Gene set enrichment analysis demonstrated that genes involved in mediating E2 response and formation of cell adhesions, tight junctions, and cytoskeletal dynamics were enriched in the gene expression dataset (Fig. S5 *G* and *H*). Thus, gene expression signatures were different between the control and *Alk3* cKO uterine luminal epithelium during the window of implantation.

Previous studies have shown that the luminal uterine epithelium undergoes dramatic morphological remodeling into a state that is permissive of blastocyst attachment/invasion (1). These changes, described as the "plasma membrane transformation," consist of decreased epithelial cell polarity, microvilli flattening, and desmosome/tight junction disassembly (2). To characterize the epithelial cell defects in the uterine epithelium of *Alk3* cKO mice further, we performed SEM (Fig. 3 *A*–*D*) and transmission electron microscopy (TEM) (Fig. 3 *E*–*H*) in the uteri of 3.5-dpc control and *Alk3* cKO mice. Both SEM and TEM analyses showed that *Alk3* cKO mice had longer and more abundant microvilli than the controls; TEM also demonstrated the presence of tight junctions in the luminal epithelium (Fig. 3*H*, yellow arrowheads). These analyses indicated the presence of morphological defects in the luminal uterine epithelium of *Alk3* cKO mice.

To characterize this defect further, we used markers of epithelial cell polarity in the 3.5-dpc uteri of control and *Alk3* cKO mice (2, 39). We used immunohistochemistry (IHC) to detect the expression of acetylated-α-tubulin, a marker of stable microtubules,

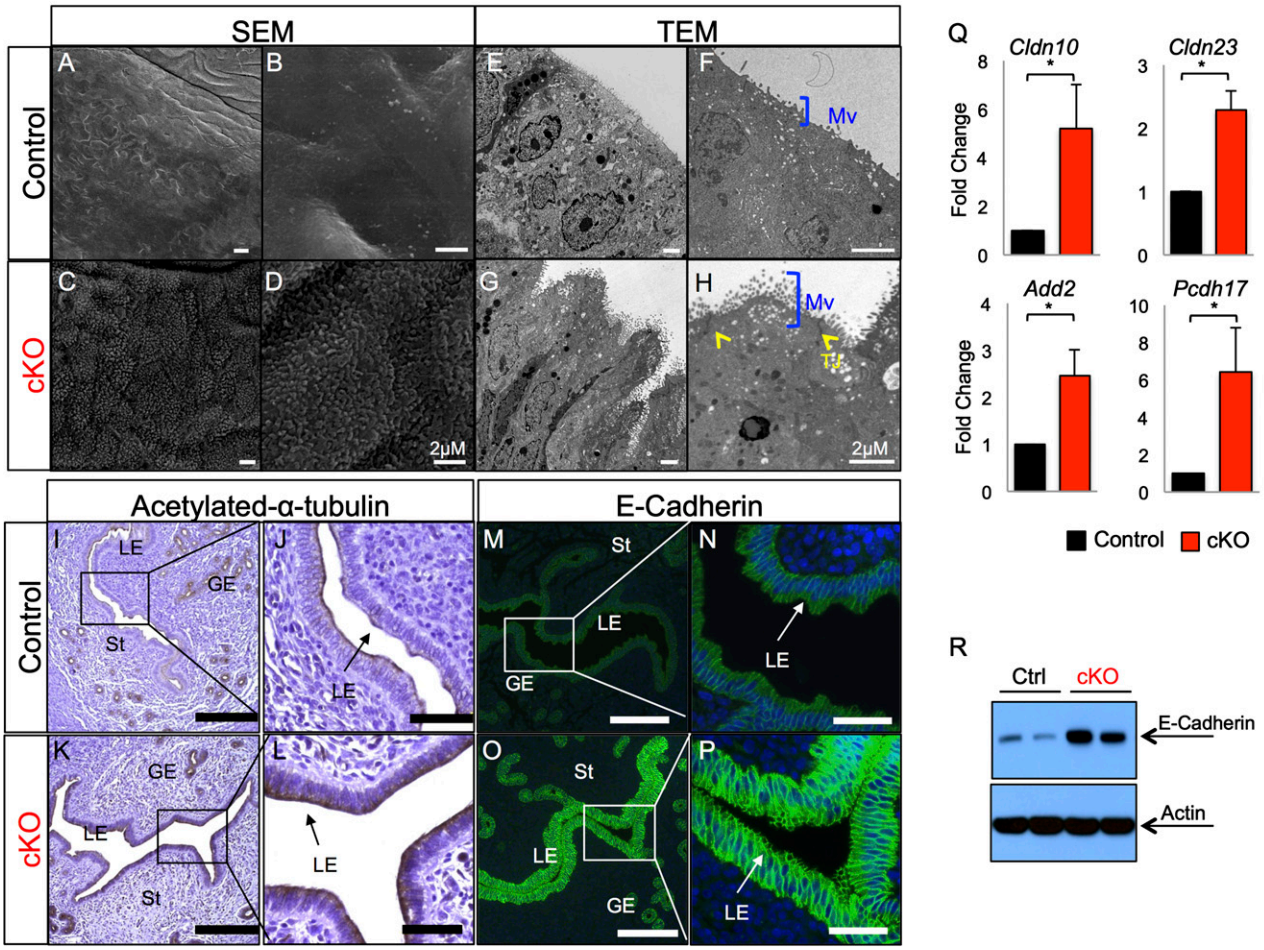

Fig. 3. ALK3 regulates luminal epithelial remodeling during the window of implantation. SEM of control (*A* and *B*) and *Alk3* cKO (*C* and *D*) uteri at 3.5 dpc is shown. TEM of the luminal uterine epithelium in the uterus of control (*E* and *F*) and *Alk3* cKO (*G* and *H*) mice at 3.5 dpc is shown. (Scale bars: 2 μM.) (Low-power images: *A*, *C*, *E*, and *G*; high-power images: *B*, *D*, *F*, and *H*). IHC of acetylated α-tubulin in the 3.5-dpc uterus of control (*I* and *J*) and *Alk3* cKO (*K* and *L*) mice is shown. (Scale bars: lower magnification, 200 μM; higher magnification, 50 μM.) E-cadherin staining on the 3.5-dpc uterus of control (*M* and *N*) and *Alk3* cKO (*O* and *P*) mice is shown. (Scale bars: lower magnification, 200 μM; higher magnification, 40 μM.) (*Q*) qRT-PCR of genes involved in tight junction formation and cytoskeletal dynamics in the luminal epithelium of 3.5-dpc control and *Alk3* cKO mice ($n = 4$). (*R*) E-cadherin immunodetection in the 4.5-dpc uterus of control and *Alk3* cKO mice. GE, glandular epithelium; Mv, microvilli (blue bracket); TJ, tight junctions (yellow arrowheads). *$P < 0.05$. Data are mean ± SEM.

and observed stronger expression in the luminal epithelium of the cKOs (Fig. 3 *I–L*). Likewise, the expression of E-cadherin, a marker of cell polarity and cell junctions, was more intense in the cKOs (Fig. 3 *M–P*). We also observed that the expression of genes involved in cell junctions, such as claudin 10 (*Cldn10*) and *Cldn23*, and cytoskeletal dynamics, such as adducin 2 (*Add2*) and protocadherin 17 (*Pcdh17*), were more highly expressed in the luminal epithelium of the cKOs at 3.5 dpc (Fig. 3*Q*). A Western blot confirmed that this increase in E-cadherin persisted in the uterus at 4.5 dpc (Fig. 3*R*). Overall, these results demonstrated structural defects in the luminal epithelium of the *Alk3* cKO mice during the window of implantation.

Enhanced E2 Receptor Signaling in the Uterus of Alk3 cKO Mice. The transition of the luminal uterine epithelium from the nonreceptive phase to the receptive phase is coordinated by the action of the steroid hormones E2 and P4. Our microarray analysis indicated differences in the expression of E2-related genes between control and *Alk3* cKO mice (Fig. S5 *F* and *G*). To validate this result, we analyzed the uterine expression of estrogen receptor α (ERα) and several downstream signaling targets at 3.5 dpc (Fig. 4). We detected strong ERα expression in the luminal epithelium of the *Alk3* cKO mice, which was weaker in the controls (Fig. 4 *A–D*). Immunostaining of phosphorylated histone H3 (Ser10) demonstrated increased proliferation of the luminal epithelial cells in the uteri of the *Alk3* cKO mice (Fig. 4 *E–H*). We also detected increased expression of *Esr1* and of several E2-mediated genes, such as fibroblast growth factor 2 (*Fgf2*), fibroblast growth factor 18 (*Fgf18*), aquaporin 8 (*Aqp8*), and mucin 1 (*Muc1*), in the luminal epithelium from uteri of 3.5-dpc *Alk3* cKO mice (Fig. 4*I*). Expression of *cyclin D1* (*Ccnd1*) was also significantly increased in the luminal epithelium of the *Alk3* cKO uteri (Fig. 4*I*).

Response to E2 in the uterus is highly regulated during the window of implantation (20). Although E2 is necessary to prepare the uterus for implantation, excessive E2 response prematurely closes the window of implantation (20). COUP-TFII decreases uterine E2 response during the window of implantation by inhibiting ERα activity (22). This inhibition is driven by P4, which activates Indian hedgehog, Patched (*Ptch*), and Smoothened (*Smo*), which are upstream regulators of COUP-TFII (21). However, IHC analysis of COUP-TFII or PR and gene expression of *Nr2f2* (COUP-TFII), *Ihh*, and *Smo* failed to detect significant differences between controls and cKO mouse uteri at 3.5 dpc and 4.5 dpc (Fig. S6). We also measured the gene and protein levels of HAND2, a key transcription factor that inhibits luminal epithelial proliferation during the window of implantation (23). qRT-PCR analysis of control and *Alk3* cKO uteri showed a slight but significant reduction in *Hand2* expression at 4.5 dpc (0.47 ± 0.08; $P < 0.004$) but not at 3.5 dpc (Fig. S6 *B* and *C*); however, immunostaining of HAND2 did not detect any significant differences between control and *Alk3* cKO mice (Fig. S6*A*). These results indicated that the abnormal response to E2 was independent of COUP-TFII activity.

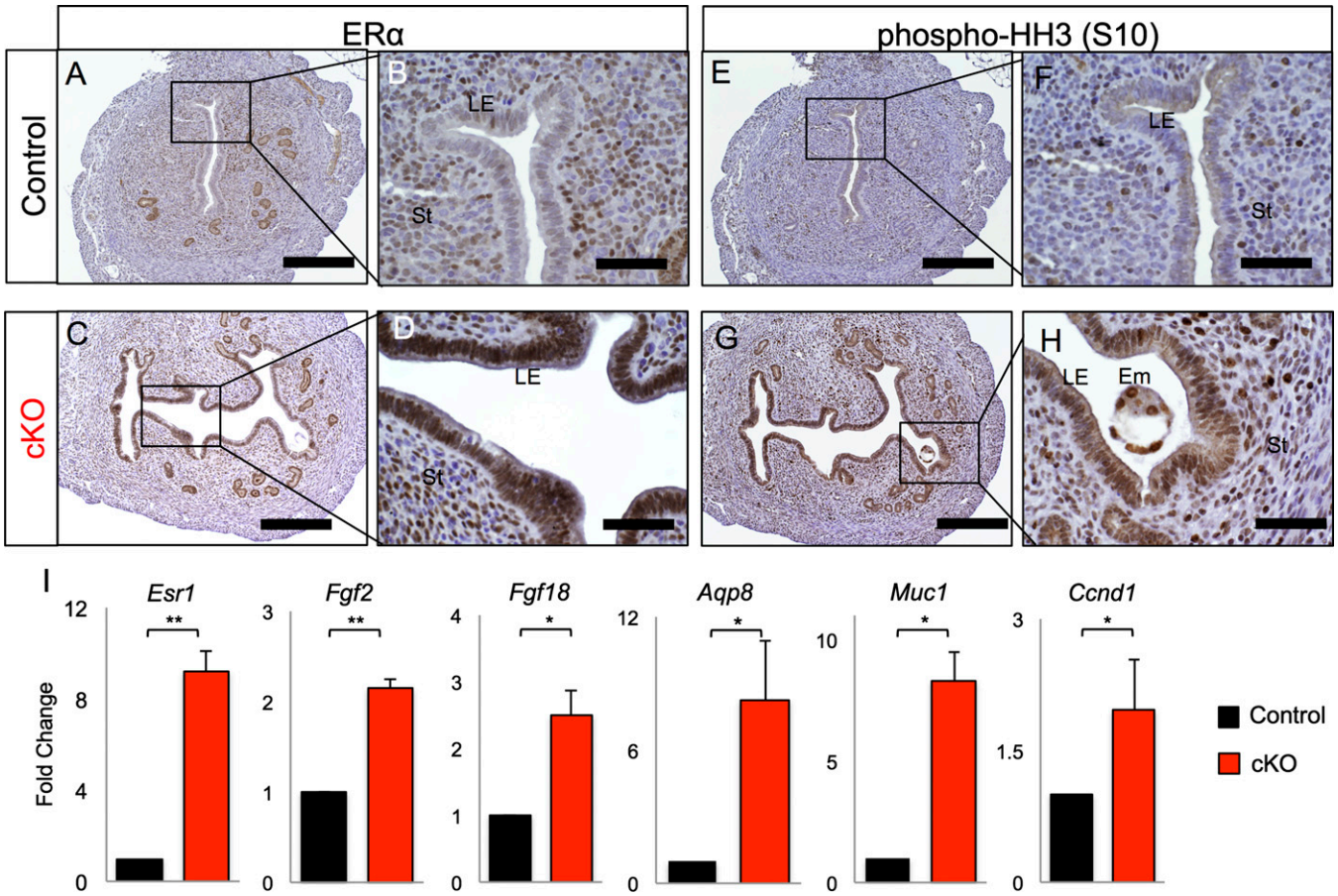

Fig. 4. Elevated E2 signaling in the uterus of *Alk3* cKO mice during the window of implantation. Immunodetection of ERα in the uterus of control (*A* and *B*) and *Alk3* cKO (*C* and *D*) mice at 3.5 dpc is shown. Immunodetection of phosphorylated histone H3 (phospho-HH3) in the control (*E* and *F*) and *Alk3* cKO (*G* and *H*) uteri is shown. (Scale bars: lower magnification, 200 μM; higher magnification, 50 μM.) (*I*) qRT-PCR analysis of E2-regulated genes in the luminal uterine epithelium of 3.5-dpc control (black bars) or *Alk3* cKO (red bars) mice ($n = 4$). *$P < 0.05$; **$P < 0.001$. Data are mean ± SEM.

KLF15 Expression Is Decreased in *Alk3* cKO Mice During the Window of Implantation. Previous studies demonstrated that proliferation of the uterine luminal epithelium is tightly regulated by the transcription factors KLF4 and KLF15 (24). KLF4 increases in response to E2, whereas KLF15 expression increases after E2 + P4 treatment. KLF4 and KLF15 regulate the transcriptional activation and repression of the *Mcm2* and *Mcm7* genes, respectively. MCM2 and MCM7 are part of the DNA replication licensing machinery that drives cell cycle progression from G1 to S phase. We subjected control and *Alk3* cKO mice to E2 and P4 treatments to induce artificial pregnancy as described in Fig. 5*A* (24). Following the last E2 + P4 injection, we collected uteri and observed increased phosphorylated histone H3 (Fig. 5 *B* and *C*) and decreased KLF15 (Fig. 5 *D* and *E*) immunoreactivity in the luminal epithelium of *Alk3* cKO mice. Gene expression analysis of the uteri indicated that *Klf15* expression was decreased, whereas *Klf4*, *Mcm2*, and *Mcm7* were significantly increased (Fig. 5*F*). The expression of cyclin-dependent kinase 2 (CDK2), CDK4, and CDK7 (*Cdk2*, *Cdk4*, and *Cdk7*) and of cyclin e1 and cyclin e2 (*Ccne1* and *Ccne2*) was significantly increased in the luminal epithelium of *Alk3* cKO mice (Fig. S7 *A* and *B*). Cyclin E/CDK2 complexes are activated during specific cell cycle phases and are required for the G1/S transition (40, 41). We also observed that phosphorylated ERα and its downstream targets, *Lcn2* and *Ltf*, were increased in the luminal epithelium of *Alk3* cKO mice (Fig. S7 *C*–*E*). Thus, in *Alk3* cKO mice, P4 does not attenuate luminal epithelial cell proliferation or E2 action, likely due to decreased KLF15 expression.

SMAD4 and PR Regulate the Expression of KLF15 in the Mouse Uterus. BMPs initiate an intracellular signaling cascade that results in the activation and nuclear translocation of SMAD1/5/8 and SMAD4 (17). SMAD1/5/8 and SMAD4 are transcription factors that are enriched at GCCT or CTCT consensus DNA sequences. We analyzed a recently published SMAD4 ChIP-sequencing (Seq) dataset (42) and identified that SMAD4 bound to the promoter and intron regions of the *Klf15* gene (Fig. 5*G*). Because KLF15 is activated by P4, we also mined a PR ChIP-Seq dataset (43) and identified that PR and SMAD4 bound to overlapping regions on intron 2 of *Klf15* (Fig. 5*G*). We also observed the presence of SMAD binding elements (GTCT) and a progesterone receptor element (PRE) half-site (TGTTTC) in this region (Fig. 5*G*). We performed PR and SMAD4 ChIP, followed by qPCR, to confirm SMAD4 and PR binding on *Klf15*. We used uteri from 3.5-dpc WT mice and performed immunoprecipitations with SMAD4 and PR Abs. As shown in Fig. 5*H*, both PR and SMAD4 were significantly enriched on intron 2 of *Klf15*, whereas no binding was detected in the genomic regions upstream (−1,000 bp, −2,000 bp) or downstream (+1,000 bp, +2,000 bp) of the *Klf15* gene (Fig. 5*H*). These results indicate that both PR and SMAD4 are required for the transcriptional regulation of *Klf15* during the window of implantation.

Discussion

Previous studies demonstrated that BMP signals are important during various stages of pregnancy. For example, BMP2 and ALK2 are required for normal endometrial stromal cell decidualization

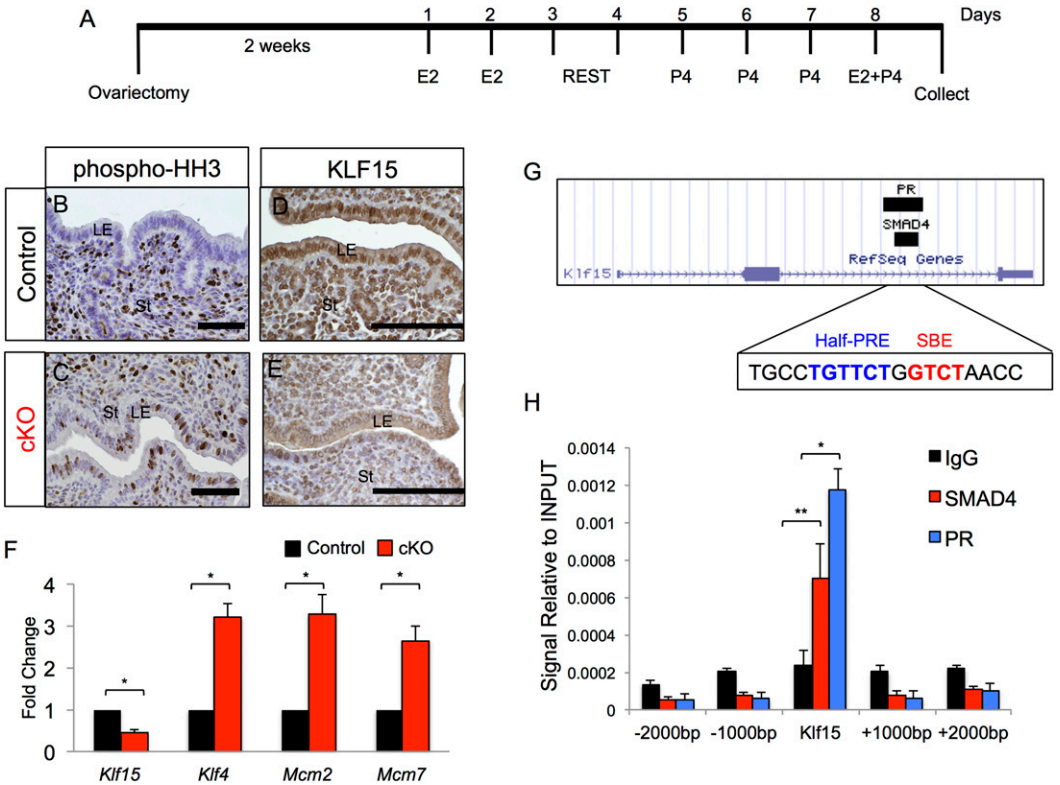

Fig. 5. SMAD4 and PR inhibit luminal epithelial cell proliferation via KLF15. (*A*) Experimental scheme used to induce artificial pregnancy in control and *Alk3* cKO mice. Immunodetection of phospho-HH3 in control (*B*) and *Alk3* cKO (*C*) mice is shown following induction of artificial pregnancy. Immunodetection of KLF15 in the uterus of control (*D*) and *Alk3* cKO (*E*) mice is shown. (Scale bars: *B* and *C*, 50 μM; *D* and *E*, 100 μM.) (*F*) qRT-PCR analysis of luminal uterine epithelium isolated from control and *Alk3* cKO mice subjected to artificial pregnancy treatments ($n = 3$). (*G*) Image obtained from the UCSC Genome Browser indicating the ChIP-Seq intervals on the *Klf15* gene for SMAD4 (chr6: 90420971–90421737) and PR (chr6: 90420636–90421879). The blue sequence indicates the half-PRE (TGTTCT), and the red sequence indicates the SMAD binding element (GTCT). (*H*) SMAD4 and PR ChIP-qPCR performed in the uteri of 3.5-dpc WT female mice. Amplified DNA regions correspond to the predicted SMAD4 and PR binding sites on *Klf15* and regions 1,000 bp and 2,000 bp upstream and downstream of *Klf15*. Data were normalized to INPUT ($n = 5$). *$P < 0.05$; **$P < 0.001$. Data are mean ± SEM.

and during postimplantation embryo development (11, 12). BMPR2 regulates important processes at midgestation, such as spiral artery remodeling and uterine natural killer cell infiltration (13). It was recently demonstrated that conditional deletion of TGF-β type 1 receptor/ALK5 in the female reproductive tract with *Pgr-cre* resulted in severe pregnancy defects, including abnormal implantation, decreased uterine natural killer cell infiltration, and defective spiral artery remodeling (44). Likewise, conditional deletion of Nodal with *Pgr-cre* leads to intrauterine growth restriction and placental defects (45).

Here, we discovered that conditional deletion of the BMPR1, ALK3, prevented pregnancy during the early stages of embryo attachment and implantation. Our results indicated that failure of embryo attachment in *Alk3* cKO mice was due to failed remodeling of the uterine epithelial cells into a state that is receptive for embryo implantation. The uterine epithelial cell defects included loss of microvilli retraction, increased epithelial cell polarity, elevated response to E2, and increased cell proliferation (Figs. 3 and 4). Ovarian E2 induces epithelial cell proliferation during proestrus, which is opposed by the rising P4 levels following copulation in preparation for embryo implantation. On day 4 of pregnancy, implantation is induced by a surge of nidatory E2 (46, 47). Previous studies demonstrated that the uterine response to E2 is highly regulated during the window of implantation (20, 22, 48). We observed elevated expression of phosphorylated ERα and its target genes in the uteri of *Alk3* cKO mice during the time of implantation (Fig. 4), indicating that the uterus was nonreceptive to an implanting blastocyst.

Our studies showed that the transition of a nonreceptive uterus to a receptive uterus requires ALK3. As summarized in Fig. 6, remodeling of the endometrium to support embryo attachment and implantation involves attenuation of E2 signaling and increased P4 signaling. Our results indicated that BMP signals mediated via ALK3 directed the structural remodeling of the luminal uterine epithelium, decreased E2 signaling in the luminal epithelium, and activated KLF15 expression (Fig. 6*B*). We also observed that coregulation of *Klf15* by SMAD4 and PR is necessary to suppress uterine epithelial proliferation, a key requirement for embryo implantation.

KLF15 is a transcription factor that directly opposes uterine luminal epithelial cell proliferation during the window of implantation (24). KLF15 regulates the transcription of the DNA replication licensing gene *Mcm2*, thereby blocking DNA synthesis and inhibiting uterine epithelial cell proliferation (24). In the luminal uterine epithelium, the expression levels of KLF4 and KLF15 increase in response to E2 and P4, respectively. E2 induction of KLF4 results in KLF4 binding to the *Mcm2* promoter, which leads to G1/S transition, DNA synthesis, and mitosis. Conversely, in the presence of E2 and P4, KLF15 is active, resulting in repression of the DNA licensing machinery and opposed cell proliferation. We observed that *Klf15* mRNA was significantly decreased in ovariectomized *Alk3* cKO mice treated with E2 and P4 to induce artificial pregnancy. This decrease in *Klf15* correlated with increased epithelial cell proliferation in the luminal uterine epithelium of the *Alk3* cKO mice. We also observed that *Klf4*, *Mcm2*, and *Mcm7* were increased in the epithelium of the *Alk3* cKO mice (Fig. 5). Thus, similar to P4, BMP signals via ALK3 to inhibit uterine epithelial cell proliferation during the window of implantation.

Using previously published SMAD4 (42) and PR (43) ChIP-Seq data, we identified that overlapping SMAD4 and PR binding sites were present in the *Klf15* gene. Analysis of these binding sites indicated the presence of half-PREs (TGTTCT) and several BMP-responsive elements (GCCG) and SMAD binding elements (GTCT). We confirmed that SMAD4 and PR bound to *Klf15* using ChIP-qPCR in uteri of 3.5-dpc mice, the window of implantation when uterine epithelial cell proliferation is inhibited. This result indicated an interaction between SMAD4 and PR that is necessary for the transcriptional regulation of *Klf15*.

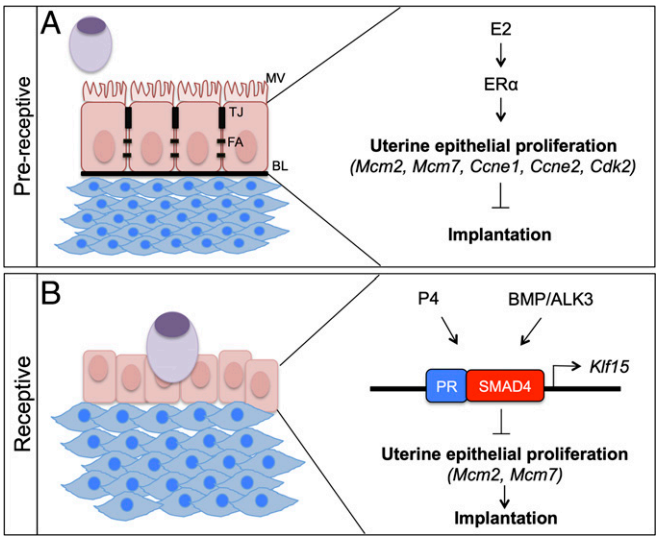

Fig. 6. Model describing the role of ALK3 during the window of implantation. (*A*) In the prereceptive state, the luminal epithelium is characterized by the presence of microvilli (MV), tight junctions (TJ), focal adhesions (FA), and an intact basal lamina (BL). During this state, E2 signaling via ERα is predominant and stimulates the proliferation of uterine luminal epithelial cells via *Mcm2, Mcm7, Ccne1, Ccne2,* and *Cdk2*. (*B*) During the receptive phase, the luminal uterine epithelium stops proliferating and the embryo penetrates into the endometrial stroma, where it stimulates decidualization. P4 signaling is dominant during this phase. BMP signaling via ALK3 is required for uterine receptivity. SMAD4 and PR bind to the same region of *Klf15* and inhibit the DNA replication licensing genes, *Mcm2* and *Mcm7*. Overall, coregulation by SMAD4 and PR inhibits the proliferation of the uterine epithelium, allowing embryo implantation.

Further studies are necessary to characterize whether SMAD4 and PR are in direct contact, and whether they jointly regulate additional genes in the uterus during the window of implantation.

Although our study only analyzed the proximal binding of SMAD4 to the *Klf15* gene, other studies suggest that the genome-wide binding patterns of SMADs include proximal promoter regions and distal enhancer regions. For example, Liu et al. (42) performed SMAD4 ChIP-Seq in mouse lungs and discovered that 25% of binding sites mapped ±1 kb of transcription start sites, but that a higher percentage (29%) of binding sites mapped to distal intergenic regions. Similarly, results from a SMAD1/5 ChIP-Seq study performed in mouse ES cells indicated that binding of a SMAD1/OCT4/SOX2 complex was located to enhancer regions (49). Another study reported similar binding patterns, in which ~85% of all SMAD1/5 binding events occurred in distal enhancer regions in human umbilical vein endothelial cells and pulmonary arterial smooth muscle cells (50). Because genome-wide SMAD1/5 binding experiments have not been performed in uterine tissues, further studies are needed to establish the genome-wide binding patterns of SMAD1, SMAD4, and SMAD5 during the window of implantation.

Our results suggest that ALK3 is necessary during the transition from the E2-dominant phase to the P4-dominant phase, which is permissive for embryo attachment and invasion. Although ALK3 is expressed in both the endometrial epithelium and stroma during early pregnancy, we observe major defects in the luminal uterine epithelium. We believe that these pronounced luminal epithelial cell defects impair embryo attachment and stromal invasion in *Alk3* cKO mice. In particular, increased ERα expression in the luminal epithelium and the elevated expression of its downstream targets are defects that contribute to the infertility of the *Alk3* cKO mice.

There are several possible explanations for the elevated E2 response observed in *Alk3* cKO mice during pregnancy. First, it is possible that ALK3 signaling induces SMAD1/5 interaction and repression of ERα, either in the cytoplasm or at the promoter regions of its target genes. Such direct interactions between SMAD1/SMAD3 and ERα have been previously reported (51, 52). Second, as demonstrated for *Klf15*, it is possible that dual transcriptional regulation by SMAD4 and PR at target genes is necessary to oppose E2 action on the uterus. PR binding studies in the uterus indicate that SMAD1/5 and SMAD4 binding motifs are significantly enriched in PR target genes (43), and thus it is likely that PR and SMAD4 may frequently bind similar target genes.

Although we observed an absence of endometrial stromal cell decidualization in the *Alk3* cKO mice following artificial induction of decidualization (Fig. S4), we observed a few decidual cells in the stroma adjacent to the embryo during natural pregnancy (Fig. 2 *E* and *F*). We believe that the embryo's contact with the uterine epithelium was likely sufficient to trigger the decidual response in the *Alk3* cKOs. However, the absence of embryo attachment and invasion, as well as the absence of BMP signals through ALK3, did not support further decidualization of the endometrial stroma and resulted in a blunted decidual response. Thus, the artificial decidualization model provided information regarding the decidual response of the *Alk3* cKO uterus to hormones and a mechanical stimulus. However, natural pregnancy indicated that growth factor signals (e.g., BMPs) or mechanical signals elicited by the attaching embryo provide a stimulus that is not provided by the artificial model.

Previous studies demonstrated the expression of various BMPs in the uterus. BMP2 is highly expressed in the mouse endometrium surrounding the implanting embryo and in the decidual tissues (18). Although BMP2 cKO mice are infertile, embryos achieve implantation and do not phenocopy the defects observed in the *Alk3* cKO mice (12, 19). This finding indicates that BMP2 is not the ligand for ALK3 during implantation or that other BMPs compensate for its absence. During implantation, BMP7 is expressed in the endometrial stroma surrounding the embryo, whereas BMP5 is weakly expressed in the uterine stroma near the myometrium (18, 53). Thus, it is plausible that BMP7, BMP5, or a combination of these ligands may drive the transition of the luminal uterine epithelium into the receptive phase. Future studies are needed to determine the physiological ligand for ALK3 during implantation.

Despite the increased use of ART in the clinic, failure rates remain high: Of the 151,923 procedures performed in 2011, only 47,818 (about 31%) resulted in live-birth deliveries (30). Implantation failure is one of the various factors contributing to the failure of ART interventions (54). The process of embryo implantation requires communication between the maternal endometrium and the implanting embryo. This bidirectional communication depends on hormones, growth factors, cytokines, and cell surface receptors (3). Improving the success of current reproductive medicine will require an understanding of the bidirectional maternal and embryonic signaling pathways. Data from our studies demonstrate the importance of signaling via ALK3 in the uterine luminal epithelium in the establishment of pregnancy. In particular, our studies demonstrate the crucial role for ALK3 in the preparation of the luminal uterine epithelium for blastocyst attachment. We believe that our data and future studies of the *Alk3* cKO mice that we generated will be useful for studying the biological mechanisms in female infertility.

Methods

Mouse Strains and Breeding Scheme to Generate Alk3 cKO Female Mice. Mice carrying the *Alk3* floxed allele were previously generated by Yuji Mishina, University of Michigan, Ann Arbor, MI, and Richard Behringer, University of Texas, MD Anderson Cancer Center, Houston (28). Briefly, *loxP* sites were inserted into the *Alk3* locus spanning exon 2, which encodes a portion of the extracellular domain. To generate *Alk3* cKO mice, $Alk3^{flox/flox}$ mice were bred to mice carrying the *Pgr-cre* knock-in allele ($Pgr^{cre/+}$) (29) to obtain $Alk3^{flox/flox}$ $Pgr^{cre/+}$ females (cKO mice). Mice were genotyped by PCR analysis using genomic tail DNA with the primers listed in Table S1 using the conditions described by Mishina et al. (28) and Soyal et al. (29). The mice were maintained on a hybrid C57BL/6J and 129S5/SvEvBrd genetic background. Animal handling and studies were performed following the NIH *Guide for the Care and Use of Laboratory Animals* (55) and were approved by the Institutional Animal Care and Use Committee of Baylor College of Medicine.

Fertility Analyses. Fertility of $Alk3^{flox/flox}$ and *Alk3* cKO mice was monitored over the course of 6 mo. The fertility studies were performed by mating *Alk3* control and *Alk3* cKO female mice with WT males for 6 mo. Normal mating was observed in the *Alk3* cKO female mice by monitoring the cages the daily for the presence of vaginal plugs, as well as the total number of pups and litters delivered.

Histological Analyses. Uteri were removed from mice and fixed in 10% (vol/vol) formalin overnight, followed by dehydration in 70% (vol/vol) ethanol. Tissues were processed for paraffin embedding in the Pathology and Histology Core Facility at Baylor College of Medicine. Paraffin sections were then stained with H&E (Electron Microscopy Sciences) or with periodic acid Schiff (Sigma) following the manufacturer's conditions. To visualize implantation sites, *Alk3* control and cKO females were mated to WT males and injected with Chicago Sky Blue Dye at 4.5 dpc as described (56). Implantation sites from controls or uteri from cKO females were then collected and processed for histology or mRNA analysis.

Tissue Collection for Protein or mRNA Extraction and qRT-PCR. Uterine tissues were collected and immediately frozen in dry ice. For protein extraction, the tissue was ground with a pestle in T-PER buffer (Pierce) with a protease inhibitor mixture (Roche). RNA was extracted using the QIAGEN RNEasy Kit by homogenizing the tissue with an OMNI-TH disrupter following the manufacturer's protocol. RNA (1–2 μg) was transcribed to cDNA using qScript cDNA Supermix (Quanta). cDNA was then used to amplify specific primers (listed in Tables S2 and S3) using SYBR Green (Life Technologies/ABI) on a Roche 480 Light Cycler II. Data were analyzed using the ΔΔCt method as described (57) and analyzed using a Student's *t* test or ANOVA analyses with Tukey's multiple comparison posttests using Prism GraphPad version 7.

Separation of Uterine Epithelial and Stromal Cells. To obtain epithelial and stromal uterine cells, mice were mated and their uteri were collected 3.5 dpc. We used the conditions described by Clementi et al. (11) to obtain epithelial and/or stromal cells from the uterus. Briefly, uteri were collected and cut into 2- to 5-mm cross-sections, followed by incubation in 1% trypsin solution in HBSS. After a 30-min incubation at 37 °C, the epithelial cells were mechanically separated from the uterus using forceps and a mouth pipette. Purity of the epithelial cells was determined by analyzing *Krt8* and *Vim* mRNA and protein levels using qRT-PCR and immunofluorescence, respectively.

Hormone Treatments. Mice were subjected to artificial pregnancy by timed hormone injections as described (24). Briefly, 6-wk-old mice were ovariectomized, allowed 2 wk of recovery, primed with 100 ng of E2 (in sesame oil), rested for 2 d, and then divided into four groups and injected with the following hormone regimen for 4 d: (*i*) injected with oil, (*ii*) injected with 50 ng of E2 on day 4, (*iii*) injected with 1 mg of P4 on days 1–4, and (*iv*) injected with 1 mg of P4 on days 1–3 and then with 1 mg of P4 + 50 ng of E2 on day 4. Mouse uteri were collected 15 h following the last injection. RNA was isolated from whole uteri, fixed in formalin, or processed for epithelial/stromal cell isolation. To induce superovulation in mice, 3-wk-old female control and *Alk3* cKO females were injected with 5 international units of PMSG. Forty-eight hours later, the ovaries were collected, processed for histology, and analyzed for the presence of follicles.

ACKNOWLEDGMENTS. We thank Drs. Yuji Mishina and Richard Behringer for their kind gift of the $Alk3^{flox/flox}$ mice. These studies were supported by Eunice Kennedy Shriver National Institute of Child Health and Human Development Grants HD032067 (to M.M.M.) and HD042311 (to J.P.L.), Institutional Research and Academic Career Development Award K12-GM084897 (to D.M.), National Cancer Institute Grant CA125123 (to C.J.C.), and the A. I. & Manet Schepps Endowment for Discovery (to D.M. and M.M.M.).

1. Kaneko Y, Lindsay LA, Murphy CR (2008) Focal adhesions disassemble during early pregnancy in rat uterine epithelial cells. *Reprod Fertil Dev* 20(8):892–899.
2. Kaneko Y, Day ML, Murphy CR (2013) Uterine epithelial cells: Serving two masters. *Int J Biochem Cell Biol* 45(2):359–363.
3. Wang H, Dey SK (2006) Roadmap to embryo implantation: Clues from mouse models. *Nat Rev Genet* 7(3):185–199.
4. Vasquez YM, DeMayo FJ (2013) Role of nuclear receptors in blastocyst implantation. *Semin Cell Dev Biol* 24(10-12):724–735.
5. Katagiri TST, Miyazono K (2008) *The Bone Morphogenetic Proteins* (Cold Spring Harbor Laboratory Press, Plainview, NY).
6. Peng J, et al. (2015) Uterine activin receptor-like kinase 5 is crucial for blastocyst implantation and placental development. *Proc Natl Acad Sci USA* 112(36): E5098–E5107.
7. Li Q, et al. (2011) Transforming growth factor β receptor type 1 is essential for female reproductive tract integrity and function. *PLoS Genet* 7(10):e1002320.
8. Pangas SA, Matzuk MM (2008) *The TGF-β Family in the Reproductive Tract* (Cold Spring Harbor Laboratory Press, Plainview, NY).
9. Dong J, et al. (1996) Growth differentiation factor-9 is required during early ovarian folliculogenesis. *Nature* 383(6600):531–535.
10. Li Q, et al. (2008) Redundant roles of SMAD2 and SMAD3 in ovarian granulosa cells in vivo. *Mol Cell Biol* 28(23):7001–7011.
11. Clementi C, et al. (2013) Activin-like kinase 2 functions in peri-implantation uterine signaling in mice and humans. *PLoS Genet* 9(11):e1003863.
12. Lee KY, et al. (2007) Bmp2 is critical for the murine uterine decidual response. *Mol Cell Biol* 27(15):5468–5478.
13. Nagashima T, et al. (2013) BMPR2 is required for postimplantation uterine function and pregnancy maintenance. *J Clin Invest* 123(6):2539–2550.
14. Ducy P, Karsenty G (2000) The family of bone morphogenetic proteins. *Kidney Int* 57(6):2207–2214.
15. Miyazono K, Kamiya Y, Morikawa M (2010) Bone morphogenetic protein receptors and signal transduction. *J Biochem* 147(1):35–51.
16. Matzuk MM, Burns KH (2012) Genetics of mammalian reproduction: modeling the end of the germline. *Annu Rev Physiol* 74:503–528.
17. Massagué J, Seoane J, Wotton D (2005) Smad transcription factors. *Genes Dev* 19(23): 2783–2810.
18. Paria BC, et al. (2001) Cellular and molecular responses of the uterus to embryo implantation can be elicited by locally applied growth factors. *Proc Natl Acad Sci USA* 98(3):1047–1052.
19. Li Q, et al. (2007) Bone morphogenetic protein 2 functions via a conserved signaling pathway involving Wnt4 to regulate uterine decidualization in the mouse and the human. *J Biol Chem* 282(43):31725–31732.
20. Ma WG, Song H, Das SK, Paria BC, Dey SK (2003) Estrogen is a critical determinant that specifies the duration of the window of uterine receptivity for implantation. *Proc Natl Acad Sci USA* 100(5):2963–2968.
21. Kurihara I, et al. (2007) COUP-TFII mediates progesterone regulation of uterine implantation by controlling ER activity. *PLoS Genet* 3(6):e102.
22. Lee DK, et al. (2010) Suppression of ERalpha activity by COUP-TFII is essential for successful implantation and decidualization. *Mol Endocrinol* 24(5):930–940.
23. Li Q, et al. (2011) The antiproliferative action of progesterone in uterine epithelium is mediated by Hand2. *Science* 331(6019):912–916.
24. Ray S, Pollard JW (2012) KLF15 negatively regulates estrogen-induced epithelial cell proliferation by inhibition of DNA replication licensing. *Proc Natl Acad Sci USA* 109(21):E1334–E1343.
25. Knoedler JR, Denver RJ (2014) Krüppel-like factors are effectors of nuclear receptor signaling. *Gen Comp Endocrinol* 203:49–59.
26. Wade HE, et al. (2010) Multimodal regulation of E2F1 gene expression by progestins. *Mol Cell Biol* 30(8):1866–1877.
27. Mishina Y, Suzuki A, Ueno N, Behringer RR (1995) Bmpr encodes a type I bone morphogenetic protein receptor that is essential for gastrulation during mouse embryogenesis. *Genes Dev* 9(24):3027–3037.
28. Mishina Y, Hanks MC, Miura S, Tallquist MD, Behringer RR (2002) Generation of Bmpr/Alk3 conditional knockout mice. *Genesis* 32(2):69–72.
29. Soyal SM, et al. (2005) Cre-mediated recombination in cell lineages that express the progesterone receptor. *Genesis* 41(2):58–66.
30. Sunderam S, et al.; Centers for Disease Control and Prevention (CDC) (2014) Assisted reproductive technology surveillance–United States, 2011. *MMWR Surveill Summ* 63 (10):1–28.
31. Wilcox AJ, et al. (1988) Incidence of early loss of pregnancy. *N Engl J Med* 319(4): 189–194.
32. Norwitz ER, Schust DJ, Fisher SJ (2001) Implantation and the survival of early pregnancy. *N Engl J Med* 345(19):1400–1408.
33. van Mourik MS, Macklon NS, Heijnen CJ (2009) Embryonic implantation: Cytokines, adhesion molecules, and immune cells in establishing an implantation environment. *J Leukoc Biol* 85(1):4–19.
34. Achache H, Revel A (2006) Endometrial receptivity markers, the journey to successful embryo implantation. *Hum Reprod Update* 12(6):731–746.
35. Hantak AM, Bagchi IC, Bagchi MK (2014) Role of uterine stromal-epithelial crosstalk in embryo implantation. *Int J Dev Biol* 58(2-4):139–146.
36. Lim H, et al. (1997) Multiple female reproductive failures in cyclooxygenase 2-deficient mice. *Cell* 91(2):197–208.
37. Ramathal CY, Bagchi IC, Taylor RN, Bagchi MK (2010) Endometrial decidualization: Of mice and men. *Semin Reprod Med* 28(1):17–26.
38. Finn CA, Martin L (1972) Endocrine control of the timing of endometrial sensitivity to a decidual stimulus. *Biol Reprod* 7(1):82–86.
39. Daikoku T, et al. (2011) Conditional deletion of Msx homeobox genes in the uterus inhibits blastocyst implantation by altering uterine receptivity. *Dev Cell* 21(6): 1014–1025.
40. Ohtsubo M, Theodoras AM, Schumacher J, Roberts JM, Pagano M (1995) Human cyclin E, a nuclear protein essential for the G1-to-S phase transition. *Mol Cell Biol* 15(5): 2612–2624.
41. Lim S, Kaldis P (2013) Cdks, cyclins and CKIs: Roles beyond cell cycle regulation. *Development* 140(15):3079–3093.
42. Liu J, et al. (2015) ErbB2 Pathway Activation upon Smad4 Loss Promotes Lung Tumor Growth and Metastasis. *Cell Rep* 10(9):1599–1613.
43. Rubel CA, et al. (2012) Research resource: Genome-wide profiling of progesterone receptor binding in the mouse uterus. *Mol Endocrinol* 26(8):1428–1442.
44. Peng J, et al. (2015) Uterine activin receptor-like kinase 5 is crucial for blastocyst implantation and placental development. *Proc Natl Acad Sci USA* 112(36):E5098–E5107.
45. Park CB, DeMayo FJ, Lydon JP, Dufort D (2012) NODAL in the uterus is necessary for proper placental development and maintenance of pregnancy. *Biol Reprod* 86(6):194.
46. McCormack JT, Greenwald GS (1974) Evidence for a preimplantation rise in oestradiol-17beta levels on day 4 of pregnancy in the mouse. *J Reprod Fertil* 41(2):297–301.
47. Finn CA, Martin L (1974) The control of implantation. *J Reprod Fertil* 39(1):195–206.
48. Zhang S, et al. (2014) Uterine Rbpj is required for embryonic-uterine orientation and decidual remodeling via Notch pathway-independent and -dependent mechanisms. *Cell Res* 24(8):925–942.
49. Chen X, et al. (2008) Integration of external signaling pathways with the core transcriptional network in embryonic stem cells. *Cell* 133(6):1106–1117.
50. Morikawa M, et al. (2011) ChIP-seq reveals cell type-specific binding patterns of BMP-specific Smads and a novel binding motif. *Nucleic Acids Res* 39(20):8712–8727.
51. Yamamoto T, Saatcioglu F, Matsuda T (2002) Cross-talk between bone morphogenic proteins and estrogen receptor signaling. *Endocrinology* 143(7):2635–2642.
52. Matsuda T, Yamamoto T, Muraguchi A, Saatcioglu F (2001) Cross-talk between transforming growth factor-beta and estrogen receptor signaling through Smad3. *J Biol Chem* 276(46):42908–42914.
53. Erickson GF, Fuqua L, Shimasaki S (2004) Analysis of spatial and temporal expression patterns of bone morphogenetic protein family members in the rat uterus over the estrous cycle. *J Endocrinol* 182(2):203–217.
54. Timeva T, Shterev A, Kyurkchiev S (2014) Recurrent implantation failure: The role of the endometrium. *J Reprod Infertil* 15(4):173–183.
55. Committee on Care and Use of Laboratory Animals (1996) *Guide for the Care and Use of Laboratory Animals* (Natl Inst Health, Bethesda), DHHS Publ No (NIH) 85-23.
56. Deb K, Reese J, Paria BC (2006) Methodologies to study implantation in mice. *Methods Mol Med* 121:9–34.
57. Schmittgen TD, Livak KJ (2008) Analyzing real-time PCR data by the comparative C(T) method. *Nat Protoc* 3(6):1101–1108.
58. Lee TI, Johnstone SE, Young RA (2006) Chromatin immunoprecipitation and microarray-based analysis of protein location. *Nat Protoc* 1(2):729–748.